

# Anchor Distance for 3D Multi-Object Distance Estimation from 2D Single Shot

Hyeonwoo Yu and Jean Oh

*Abstract*—Visual perception of the objects in a 3D environment is a key to successful performance in autonomous driving and simultaneous localization and mapping (SLAM). In this paper, we present a real time approach for estimating the distances to multiple objects in a scene using only a single-shot image. Given a 2D Bounding Box (BBox) and object parameters, a 3D distance to the object can be calculated directly using 3D reprojection; however, such methods are prone to significant errors because an error from the 2D detection can be amplified in 3D. In addition, it is also challenging to apply such methods to a real-time system due to the computational burden. In the case of the traditional multi-object detection methods, existing works have been developed for specific tasks such as object segmentation or 2D BBox regression. These methods introduce the concept of anchor BBox for elaborate 2D BBox estimation, and predictors are specialized and trained for specific 2D BBoxes. In order to estimate the distances to the 3D objects from a single 2D image, we introduce the notion of *anchor distance* based on an object’s location and propose a method that applies the anchor distance to the multi-object detector structure. We let the predictors catch the distance prior using anchor distance and train the network based on the distance. The predictors can be characterized to the objects located in a specific distance range. By propagating the distance prior using a distance anchor to the predictors, it is feasible to perform the precise distance estimation and real-time execution simultaneously. The proposed method achieves about 30 FPS speed, and shows the lowest RMSE compared to the existing methods.

## I. INTRODUCTION

Real-time visual perception and understanding of an environment is critical to the successes of robotic applications including autonomous driving. Visual Simultaneous Localization and Mapping (SLAM), in particular, is essential for performing navigation and exploration tasks as well as supporting high-level missions that require reliable mobility. Recently, SLAM focuses on two major facets: semantic recognition and spatial understanding [1], [2], [3], [4], [5]. With the advancement of deep neural networks, several approaches have been developed to achieve highly accurate results on semantic recognition, taking advantage of rich and sophisticated semantic features and various disentangled features such as shape, orientation, or dimensions of 2D and 3D Bounding Box (BBox) [6], [7], [8], [9], [10], [11]. In this paper, we focus on real-time spatial understanding including accurate estimation of object locations specifically addressing the challenge in a monocular camera setting.

The majority of existing work on SLAM systems for autonomous driving relies heavily on an inverse reprojection

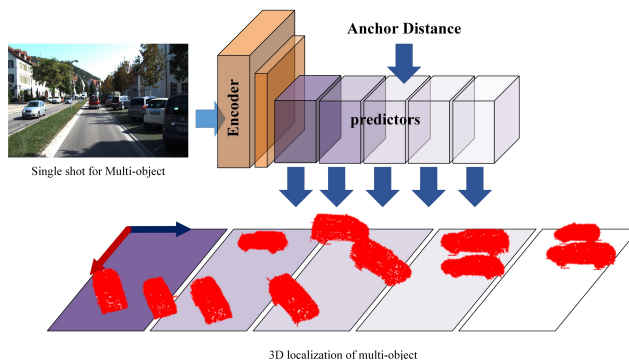


Fig. 1. The overview of the proposed method. The network estimates the distance of multi-object with multiple predictors from single image. Each predictor is specialized to the object located in specific distance range by using anchor distance. With the anchor distance, predictors are provided priors of the distance so that accurate estimation under simple and fast network structure can be achieved.

method [12], [13], [14], [15] where an optimal distance is computed by reprojecting a 3D shape or its 3D BBox to a corresponding 2D BBox. The performance of such a method, however, tends to be extremely sensitive to that of image segmentation and/or 2D BBox estimation.

Alternatively, depth estimation methods [16], [17], [18] can be utilized for object-level 3D estimation, by taking the median depth of all geometric features or pixels within the detected 2D BBox [4], [13], [19]. In these methods, however, it is hard to discard the outlier pixels especially if an object is severely occluded. Adding a segmentation method such as [20] can have minor improvements in the performance at the cost of significant computational burden; estimating the depth of object’s center from depth values of partial observation is still challenging.

To achieve robust object depth estimation, we can exploit existing single-shot, multi-object detection approaches, which are specialized in category classification, segmentation, and 2D BBox regression [20], [21], [22], [23]. Based on such methods, various approaches have been proposed for object disentangled representation [24], [25], [26], [27]. Some works on multi-object understanding use multi-object detector to obtain object region followed by a post-processing step [28], [9], [29]. Others train their baseline network with Region Proposal Network (RPN) and perform Region of Interest (RoI) pooling to obtain visual features of objects [30]. These methods deploy additional structure to estimate various object representations in addition to the baseline for multi-object detection. Such an increased

Hyeonwoo Yu and Jean Oh are with the Robotics Institute of Carnegie Mellon University, Pittsburgh, PA 15213, USA {hyeonwoy, hyaejino}@andrew.cmu.edu

complexity of the network makes real-time performance challenging [20], [28]. To simplify the structure of the network, prior knowledge of an object can be exploited. Since the purpose of the existing multi-object detector is to perform the 2D BBox regression, anchor BBoxes are used as prior knowledge of 2D BBox [23], [22], [31]. To utilize such prior knowledge represented by anchor BBoxes, several methods construct their networks by deploying multiple predictors according to anchor BBoxes. These methods, however, have limitations in learning object representations such as distance estimation as they mainly focus on the 2D BBox on the image plane.

To bridge the gap between existing multi-object detection and distance estimation, we introduce the notion of *anchor distance*. We then propose a multi-object distance estimation method specifically designed for both real-time performance and accurate estimation. Given a 2D image as an input, we aim to estimate the distance to objects in a 3D space. Our work makes the following contributions to the state-of-the-art methods:

- as shown in Fig. 1, we transform the 2D single shot to 3D spatial grids represented as predictors so that the proposed method achieves real-time performance without a 2D RoI pooling network;
- compared to existing 2D detectors, the proposed method achieves robust detection results with overlapped objects since objects are detected in 3D grid space; and
- we define and utilize the notion of anchor distance, thus predictors in our proposed network are specialized and robust to the objects in specific distance range.

When compared to the state-of-the-art method, the proposed method runs about 4 times faster at 30 FPS and shows competitive results in Abs Relative (Abs Rel) difference, and outstanding results in RMSE.

## II. RELATED WORK

In the context of mobile robot navigation, 3D object detection and localization are compulsory to perform collision avoidance, object-oriented SLAM or safe navigation in autonomous driving. In this section, we discuss related works on monocular SLAM specifically focusing on the 3D localization. Various existing works on this end adopt the idea of inverse perspective projection [13], [14], [3], [15]. The 2D projection of an object is invertible since its extent parameters resolve depth ambiguity. That is, by mapping between 2D BBoxes from an object detection module and 3D BBoxes, these approaches can estimate the distance in 3D given a 2D input image. Also, in a special setting such as autonomous driving, we can assume that the height of a camera is known and all of the objects are placed on the ground. This allows the algorithm to resolve the scale-ambiguity and estimate object location. These approaches are still based on 2D BBox regression, the quality of distance estimation is also bounded by the precision of the 2D BBoxes.

To obtain 2D perception such as 2D BBox regression, using an additional object detection method is inevitable.

Several convolutional neural network (CNN)-based algorithms have been proposed to perform multi-object detection in real time. These approaches are mainly customized for specific tasks such as detection using 2D BBox regression, object categorization, and segmentation. Because the performance of these approaches depends on the quality of 2D BBoxes inferred from an object detector, results of 2D BBox detection have been commonly used as an evaluation criterion for the overall performance [23]. This trend has led to the development of new techniques and network designs to improve the performance of 2D BBox regression [22], [31].

Existing multi-object perception techniques mainly focus on 2D BBox regression and category estimation, and their variations estimate disentangled representations such as orientation, shape, or distance of objects [7], [24], [32]. Most of the proposed methods exploit visual features to learn the complex representations of objects [6], [11], [33], [34], [35]. Therefore, by using an additional multi-object detector, 2D BBox is provided for RoI pooling in order to obtain visual features for the target region. Other methods are proposed by modifying the existing multi-object detector structure for directly extracting features and performing object understanding [36], [24], [20], [30]. However, they still deploy the RPN for RoI pooling. Moreover, it is necessary to construct the networks in addition to the baseline structure for object understanding tasks with a large variation such as depth estimation. For these networks they use structures with several drawbacks such as the increase of memory footprint to cover the non-linearity of object understanding and perform elaborate estimation [30], [32]. These methods are effective in representing specific aspects of objects, but it is challenging to apply to mobile robot systems in real-time due to their complexity.

In order to relax the network and achieve more robust results, a number of methods have been introduced to provide prior information about objects to the networks using anchors. Techniques for 2D detection exploit anchor of 2D BBox [23], [22], [31], and techniques for 3D include orientation and distance as well as 2D BBox in anchor [32], [27]. However, in these methods, anchors are still defined by clustering based on the 2D BBox of object on 2D image plane. Since various object representations such as locations, shape, or orientation are not directly proportional to the projected 2D BBox, it is not suitable to use anchors arranged with 2D BBox for learning the distance of objects. Therefore, we define anchor distance for object 3D localization and introduce a method of training networks based on the anchors that achieves real-time performance.

## III. APPROACH

In general, when a monocular camera sensor is used for recognizing an object, the location coordinates can be estimated using the mapping between the 2D object detection and both the dimension and the orientation of a corresponding 3D BBox. Assume that a 2D BBox of a detected object and the dimension and the orientation of

a 3D BBox are given or have been estimated. With the constraint that the 3D BBox fits tightly into the 2D detection box on the 2D input image, 3D coordinates of the detected object can be calculated; however, estimating 3D coordinates by overlapping the projection of 3D to 2D BBoxes usually causes inaccurate results due to the sensitivity to the size of the 2D BBoxes. A small error in the size of BBox can cause a substantial error in the distance estimation calculation. Furthermore, this approach can add a significant calculation burden, as each side of the 2D BBox can correspond to any of the eight corners of the 3D BBox. Even with the strong constraint that most of the objects are located on a ground plane, at least 64 configurations must be checked [10]. To address these challenges, we propose an approach that achieves both high accuracy and real-time performance by directly estimating the object distance.

### A. 3D Coordinate and 2D Bounding Box

Given 3D directions to the center of object and depth (or distance from origin), 3D coordinates can solely be determined. For estimating the center of the 3D object, the center of a 2D BBox can be exploited by reprojecting it to the 3D real-world coordinate. In this way, we can have a normalized ray direction vector toward the center of the 3D object from the origin. Hence, the 3D coordinate of an object can be obtained by multiplying this ray direction vector and estimated distance. The network can also be trained to directly estimate all 3D coordinates of an object. In case of using multi-object detector, however, it can be relatively advantageous to estimate the center of an object by using the predictors distributed in a grid form. Hence, it is more accurate to compute the coordinate from reprojection than learning the  $x, y$ , and  $z$  components of location directly. We design our network to train on the distance from the origin and the 2D BBoxes as in [21], [31].

### B. Anchor Distance

In order to achieve the real-time multi-object distance estimation, our proposed method is based on a simple multi-object detection structure, namely, YOLOv2 [21]. As the existing network only estimates the center and dimensions of a 2D BBox, we let our network predict the distance from the origin of the object as well. The following problem, however, still remains: the purpose of conventional detectors is to estimate the 2D BBoxes rather than the distances to the objects, and each predictor are dedicated to learn for the corresponding BBoxes of different sizes. To reduce such a burden of the network, a 2D anchor BBox is applied to each predictor as the prior knowledge about the 2D BBox sizes. These approaches reduce the variation of the 2D BBoxes that each predictor should predict, resulting in more accurate 2D BBox estimation.

In order to achieve 3D coordinate estimations of multiple objects, we introduce the concept of anchor distance that is similar to the anchor BBox. To obtain the prior knowledge of the distance in a simple manner, the average distance corresponding to each anchor BBox can be defined by using

TABLE I  
VARIANCE OF THE DISTANCE OF 2D BBOX GROUPS AND DISTANCE GROUPS FOR KITTI DATASET

# of predictors (groups)	order	(unit : $m^2$ )	
		2D BBox grouping	distance grouping
2	1	14.84	25.69
	2	220.12	31.76
3	1	9.07	12.26
	2	33.26	8.60
	3	186.27	20.30
5	1	7.08	5.36
	2	18.68	4.27
	3	49.57	3.10
	4	91.14	9.28
	5	98.21	3.55

the average of distances of objects belonging to each anchor BBox group. Unfortunately, the size of an anchor BBox is not exactly proportional to the distance of the object. When an anchor BBox simply includes the average distance, each predictor can undesirably learn the mapping between the size of a 2D BBox and a distance. In other words, the network still learns the 2D BBox regression as its main task, leaving the burden of distance estimation to each individual predictor where the distances within a large range should still be estimated.

To address this issue, we define the concept of an anchor distance to train each predictor as follows. With an anchor distance, each predictor is specialized in estimating the distance of the object in a specific distance range, instead of being specialized in specific 2D BBoxes. Similar to obtaining the anchor BBoxes, the distances of objects are grouped through  $k$ -means clustering. Each center of the groups (or clusters) is defined as anchor distance. We compare the variance of the average distance obtained from 2D BBox clustering and that of the anchor distance from distance clustering for the case of  $k = 2, 3, 5$  in Table I. We use the `car` category in the KITTI dataset [37] as an example. The predictors are sorted by the corresponding distance in ascending order. In the case of 2D BBox grouping, the variance of the group for the long distance is greater than the one for the short distance. This is because objects that are far away from the origin are similar in terms of size of the 2D BBox. On the other hand, in the case of distance clustering, the variance is much smaller than that in the case of 2D BBox clustering for all predictors. Therefore, predictors can show more precise estimation results as they infer more consistent distances with anchor distance. The results of the network prediction using anchor distance are denoted as follows:

$$d_i = d_i^a \times \exp(t_i), \quad i \in \{0, 1, \dots, k-1\} \quad (1)$$

where  $t$  is an output of the network, and  $d^a$  is the anchor distance. Similar to [21], [31], we use an exponential function as the final activation function of the output.

In our method, the dimension of 2D BBox has no effect on distance estimation directly, but the center of 2D BBox

is crucial as it is exploited to calculate the 3D coordinate by finding the ray direction. To achieve the 2D BBox regression, priors of the BBox can be defined for our distance grouping. Simply, we can define the average BBox of clusters for anchor distance by taking the arithmetic mean of dimensions of the BBoxes. However, our clusters focus on distance so that BBoxes in a group have large variance in terms of their sizes. For more accurate BBox regression with anchor distance groups, we take the average BBox approximately where we minimize not the differences of dimensions but the differences of intersection over union (IoU) as follows:

$$(h^m)^2 = \frac{\sum w_j h_j^2}{\sum w_j}, \quad (w^m)^2 = \frac{\sum h_j w_j^2}{\sum h_j} \quad (2)$$

where  $h^m$  and  $w^m$  are the height and width of the average BBox, respectively.  $h$  and  $w$  are height and width of BBox. Using this average BBox, the network output for BBox dimension is given as:

$$\begin{aligned} h_i &= h_i^m \times \exp(u_i) \\ w_i &= w_i^m \times \exp(v_i), \quad i \in \{0, 1, \dots, k-1\} \end{aligned} \quad (3)$$

where  $u$  and  $v$  are outputs of the network. For the center of the 2D BBox, we follow the similar settings of [21].

### C. Predictors

With the anchor distance, we can provide the prior knowledge of the distance to our network. The predictor is specialized and trained for objects near specific distance as each anchor distance is assigned to each predictor of the network. As the variance of the distance inferred by a predictor decreases, the complexity of the network is decreased. The predictors of the network can construct a 3D environment without additional structures such as 3D RPN or 3D convolutional layers.

The existing multi-object detectors utilize 2D anchor BBoxes by clustering 2D BBoxes. In order to cluster 2D BBoxes, we can use the dimensions of the BBox or IoU. Likewise, anchor distance can be achieved by using various formats such as normal, squared, or log-scaled. In our work we apply all three cases to obtain the anchor distance and train the network. Whilst training, the existing multi-object detector using anchor BBox chooses the predictor that infers the closest BBox to the target BBox and assigns that target BBox to learn. Similarly, the proposed method learns the distance of the target object by selecting and training a predictor which infers the value closest to the target distance. Note that the same distance format used for obtaining anchor distance is also used when comparing the the difference between the target distance and estimated one by the predictor during training.

At the beginning of training, we found that the predictor’s inference value highly fluctuates in order to learn distances with quite large variations. In this case, objects are inconsistently assigned to the predictors regardless of the anchor distance. Therefore, during the training phase, we use the predictor’s anchor distance rather than the estimated result for predictor selection.

### D. Training Loss

In the proposed method, the distance from the origin of an object is estimated. Since a ray vector indicating the center direction of an object is obtained using a 2D BBox, all 3 components of 3D coordinate can be obtained by using distance from origin or depth. Therefore, it is possible to separately train  $x, y$ , and  $z$ . However, we assume that 2D BBox and 3D location are independent and let 2D BBox and the distance be learned separately. For the 2D BBox training, we adopt CIoU loss [38], [31]. For depth estimation,  $L_1$  loss is generally used, but in our work  $L_2$  loss is applied.

## IV. IMPLEMENTATION AND TRAINING DETAILS

To implement the proposed observation model, we use the darknet19 structure [21] for the encoder backbone. We construct the encoder by adding 3 convolutional layers with 1,024 filters followed by one convolutional layer on top of the backbone. The final convolutional layer has  $k \times (4 + 1)$  filters; 4 for 2D BBox dimensions and center, and 1 for the distance. Each predictor estimates 2D BBox and distance from the origin of the object. We pretrain the backbone network on the Imagenet classification dataset. We use the Adam optimizer with a learning rate of  $10^{-4}$ . For all training processes, a multi-resolution augmentation scheme is adopted. Similar to [21], [8], Gaussian blur, HSV saturation, RGB inversion and random brightness are applied to 2D images while training. Random scaling and translation are not used in order to preserve the 3D coordinates of objects.

## V. EXPERIMENTS

We evaluate the proposed method in various aspects. Similar to the traditional multi-object detectors, as the number of predictors increases, the estimation can be performed more precisely. In our experiments, we train the network with various numbers of predictors such as 2, 3, 5 and so on. We compare our methods to existing methods based on Faster R-CNN using RPN. A depth estimation method is also compared by using ground truth 2D BBox. We use the median depth within 2D BBox as the depth of a detected object. For the depth estimation method, we choose [16] since the method proposes ordinal regression in order to consider depth intervals. Additionally, we also implement several methods including ours in order to estimate the distance of objects - 1) *3D proj*: we implement the method that calculates distance by projecting 3D BBox in 3D space to 2D BBox on 2D image. We construct the network which shares the same backbone with our proposed method, and train the network on dimensions of 2D, 3D BBox and orientations of objects. 2) *anchor BBox*: similar to the existing detector, we evaluate the method that uses anchor BBox and average distance of groups obtained from 2D BBox clustering. In this case the average distance is calculated by taking arithmetic mean. We also evaluate the case without any distance prior. 3) *proposed method*: the proposed method using anchor distance and its training scheme is evaluated. For obtaining anchor distance by distance clustering, normal, squared, and log-scale formats are used for 3 individual models. For

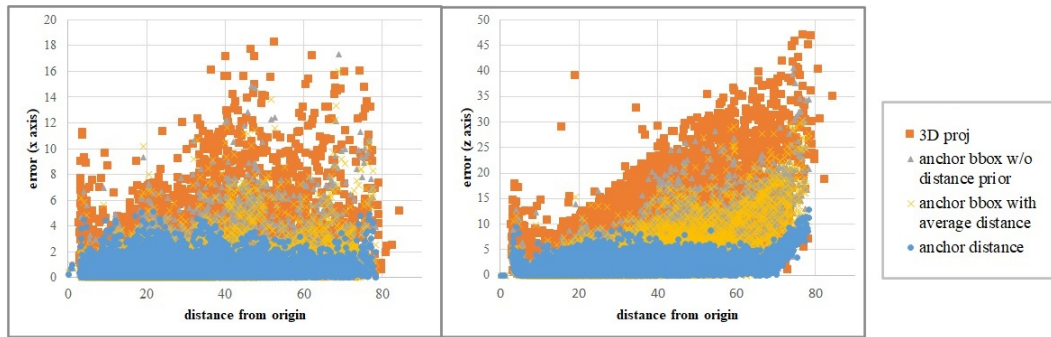


Fig. 2. Distance estimation error of  $x$  and  $z$  axes, which denote the horizontal location and depth of the object. As the distance of the object increases, the estimation error increases in case of other methods. The proposed method shows consistent error independent to the distance from origin as the method exploits the anchor distance.

each model, the same format used for anchor distance is also used for training; while choosing the predictor for the target object, target distance and estimated distances from predictors are compared by using the same format of distance that is used for clustering.

For all experiments, we use the `car` category in the KITTI 3D object detection dataset.

#### A. Relation Between Object Distance and Error

We compare the results of *3D proj*, *anchor BBox* with and without average distance, and the proposed method in Fig. 2. We plot the distance error of the object according to its distance from origin. For the method *anchor BBox* and the proposed method, we set  $k = 5$ . For the distance format of the proposed method, we use squared format. Results of  $x$  and  $z$  axis are shown, which denote horizontal and depth of the object location respectively. We leave the result of  $y$  axis out, since the height of cars have small variations compared to the depth of cars so that errors of  $y$  axis are significantly smaller than errors of the other axes. As shown in the graph, the estimation result of *3D proj* is significantly more inaccurate as the objects locate further. The further the objects are, the more similar the sizes of the 2D BBoxes are; therefore, it is challenging to infer the distance precisely since the estimations are highly sensitive to the errors of small 2D BBoxes of objects in a far distance. Compared to *3D proj*, methods using anchor BBox have more robust inferences of distance. However, as the variations are high for the distance of objects located far from the camera, it is still challenging to estimate the far distance without a tremendous error. From these results we can conclude that the distance and the 2D BBox of the object are not directly proportional to each other, but there exists a slight correlation. In the case of using anchor distance, estimations results show constant and uniform error regardless of the distance of the object.

#### B. Depth Estimation and Anchor Distance

We represent the metric evaluations of  $z$  coordinate distance (depth) estimation of the object in Table II. We follow the definitions of the metrics as in [28]. Compared to the methods based on RPN [28], [30], our method achieves a better performance in RMSE at a substantially higher frame

rate. Using depth estimation directly for object detection showed degraded performance compared to other methods as it hardly consider the overlapped or occluded states of objects.

In order to validate the anchor distance, we also evaluate the methods of 2D anchor BBox with and without average distance. As the number of predictors increases, the burden of one predictor decreases and the network can achieve the robust estimations. In other words, the more number of predictors there are, the more accurate inference is achieved. This trend is more pronounced when anchor distance is applied, and in this case the network shows significantly improved performance than when the predictors simply focus on 2D BBox.

The proposed method has the highest performance when the squared format is used, and shows the lowest performance when log-scale is used. We found that the squared distance format covers the largest range as shown in Table III. With the large range of anchor distances, the network can handle the objects distributed in various ranges efficiently. Meanwhile, in the case of 2D BBox with average distance, prior distance is the most similar to that of log-scale format. Reversely, log-scale distance grouping shows the most similar average 2D BBox to that of 2D BBox grouping; we display the 2D BBoxes of each grouping in Table IV. Therefore, we can conclude that the distance in the log-scale format is mostly related to the 2D BBox, but using the log-scale distance or 2D BBox is not sufficient to achieve the best performance as the 2D BBox is not directly proportional to the distance. In other words, using log-scale distance or 2D BBox for grouping in order to obtain prior distance is not effective. For 3D localization tasks it is better concentrating not on 2D projection, but on distance itself for defining anchors of 3D location.

#### C. Estimation Error and Execution Time

The proposed method shows a significantly better performance on the RMSE error than that of others, but in the Abs Rel metric the method does not outperform the existing method using complex structures such as ResNet or Mask-RCNN. In other words, although our proposed method is slightly inferior to the previous methods for objects that are

TABLE II  
VARIANCE OF THE DISTANCE OF 2D BBOX GROUPS AND DISTANCE GROUPS FOR KITTI DATASET

Method	FPS	# of predictors	$\sigma < 1.25$	$\sigma < 1.25^2$	Abs Rel	Sqr Rel	RMSE	RMSE <sub>log</sub>
			(higher is better)				(lower is better)	
SVR[39]	-	-	0.345	0.595	1.494	47.748	18.970	1.494
IPM[40]	-	-	0.701	0.898	0.497	35.924	15.415	0.451
Zhu et al.(ResNet50)[28]	< 15	-	0.796	0.924	0.188	0.843	4.134	0.256
Zhu et al.(VggNet16)[28]	< 15	-	0.848	0.934	0.161	0.619	3.580	0.228
Zhang et al.(MaskRCNN[ResNet50])[30]	< 7	-	0.988	-	0.051	-	2.103	-
Zhang et al.(MaskRCNN[ResNet50] + addons)[30]	< 7	-	<b>0.992</b>	-	<b>0.049</b>	-	<b>1.931</b>	-
DORN (depth map estimation) [16]	-	-	0.883	0.934	0.190	1.153	4.802	0.287
2D anchor BBox w/o distance prior	< 35	3	0.906	0.977	0.103	0.547	4.475	0.167
		5	0.911	0.981	0.096	0.474	4.225	0.157
		7	0.926	0.984	0.085	0.410	3.727	0.145
2D anchor BBox + average distance	< 35	3	0.914	0.982	0.099	0.491	4.196	0.159
		5	0.923	0.984	0.092	0.437	3.911	0.152
		9	0.949	0.988	0.094	0.344	3.401	0.144
Ours (normal anchor distance)	< 35	3	0.968	0.990	0.084	0.230	2.527	0.131
		5	0.971	0.989	0.076	0.155	1.770	0.124
		9	0.931	0.987	0.098	0.401	3.903	0.149
Ours (log-scale anchor distance)	< 35	3	0.957	0.989	0.084	0.281	3.182	0.133
		5	<b>0.972</b>	0.990	<b>0.073</b>	0.150	1.915	0.117
		9	0.952	0.988	0.092	0.313	2.936	0.142
Ours (squared anchor distance)	< 35	3	0.962	0.989	0.084	0.220	2.080	0.134
		5	0.970	0.989	0.079	0.165	<b>1.719</b>	0.127
		9						

TABLE III  
ANCHOR DISTANCE OF DIFFERENT DISTANCE FORMAT

order of predictors	(unit : m)					
	1	2	3	4	5	
anchor BBox(avr dist)	7.73	13.59	23.83	33.81	52.52	
normal	11.20	23.18	35.30	49.50	66.21	
anchor distance	log-scale	7.60	15.17	24.78	37.59	57.51
	squared	17.49	32.86	45.27	57.41	71.52

close to the origin, it is more robust when the objects are far from the origin. The structure of the proposed network is simpler than others, yet our approach using anchor distance and training scheme consistently generally achieves more accurate estimation regardless of the distance of objects.

We also present the frame rate in terms of FPS for each method. In [28], they assume that the 2D BBox regression is given in advance, so we approximately record its FPS by assuming that YOLOv2 is used. In [30], the FPS of their method is under 7, as the baseline is MaskRCNN [20] that shows 7 FPS and the method deploys additional network structure for distance estimation. The proposed network, which is based on YOLOv2 [21], however, only takes about 0.03 seconds and shows under 35 FPS for the entire estimation process. This execution time is irrelevant to the number of predictors, as adding one predictor is equivalent to adding  $(4 + 1)$  convolutional filters that only have  $(3 \times 3)$  parameters per filter. The method with 3D projection takes another 0.04 seconds after estimating 2D BBox, 3d BBox, and orientation which takes 0.03 seconds. We display the relation between RMSE error and FPS of various methods

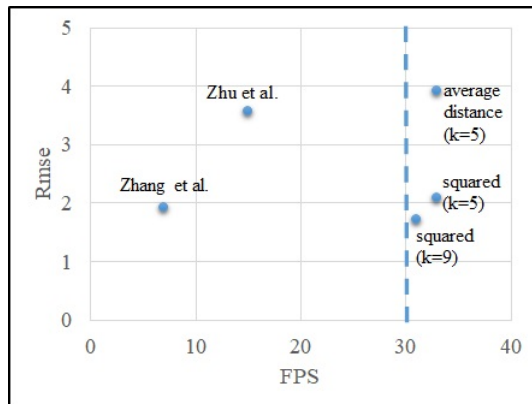


Fig. 3. The RMSE and FPS of the methods are shown. Since our method is based on a real-time detector, it demonstrates high FPS. Adopting the anchor distance as prior information compensates the simple network structure, achieving faster and better performance compared to others.

in Fig. 3.

For qualitative analysis, we display the visualization examples in Fig. 4 represented in a bird-eye view. For *3D proj*, we exploit the 2D BBox regression results from the network with  $k = 5$ . The network for *3D proj* shares the same structure of our proposed method. Also, it estimates orientations and dimensions of 2D and 3D BBox which are used for calculating distance. Here, we use a squared format for the proposed method. In *3D proj*, the error of the distance estimation increases since the size of the 2D BBox becomes similar as the objects are located far away. In the proposed method, the higher the number of predictors  $k$  is, the more accurate the estimated results are.



TABLE IV  
COMPARISON OF 2D BBOX DIMENSIONS FOR KITTI DATASET

# of predictors orders	(unit : pixel)									
	2		3			5				
	1	2	1	2	3	1	2	3	4	5
anchor box(IoU)	151/268	51/86	164/296	83/144	39/64	175/321	108/183	57/104	37/61	24/35
anchor dist(log-scale)	139/226	37/67	156/246	59/103	29/53	181/273	104/178	57/99	36/67	23/41
anchor dist(normal)	133/219	30/55	141/229	42/75	24/42	156/246	63/111	38/69	27/49	19/32
anchor dist(squared)	129/215	24/43	134/220	33/60	21/36	140/227	42/75	29/54	22/39	17/29

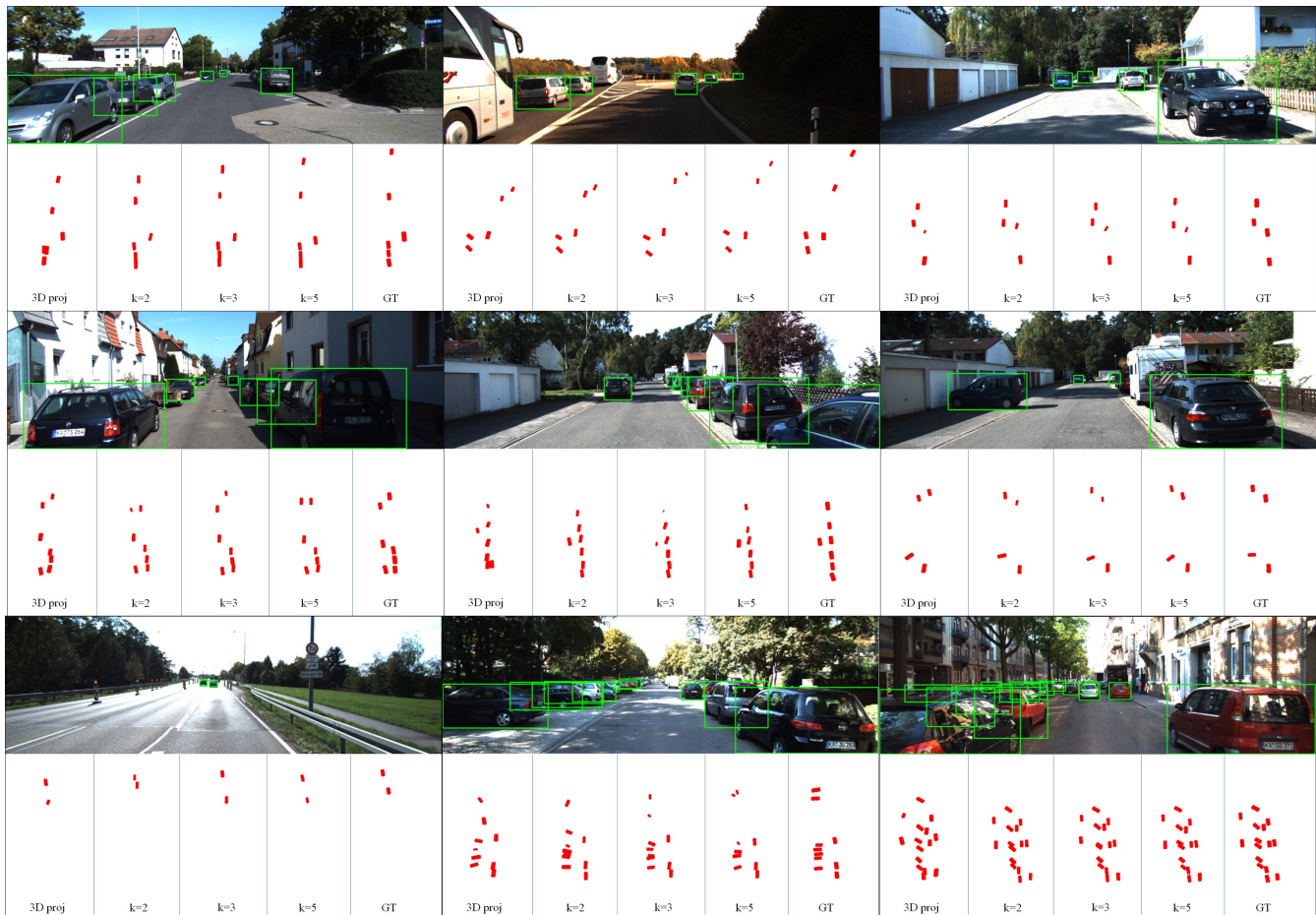


Fig. 4. Examples of the visualizations in a bird-eye view. We compare the results of using 3D projection and the results of ours with  $k = 2, 3, 5$ . Since the method using 3D projection highly depends on the 2D bounding box and orientation, it shows incorrect results for the objects located far away or occluded. The proposed method shows better performance with multiple predictors, as a number of anchor distances allows the network to estimate the results with low non-linear complexity.

## VI. CONCLUSION

We propose a multi-object distance estimation method using anchor distance. Conventional methods based on multi-object detection train their predictors based on 2D Bounding Box (BBox). Other techniques for multi-object distance estimation rely heavily on complex structure for sophisticated distance estimation. The proposed method can achieve robust estimation and real-time performance as the method selects and trains the predictors of the network based on the distance of objects. To build a prior, we define the anchor distance by clustering the objects with their distance in various formats such as squared or log-scaled. The anchor distance gives

predictors a strong prior knowledge of distance. Predictors are dedicated to learning objects in a specific distance range according to their anchor distances. Because the proposed method trains the network based on distance, it is able to achieve more accurate estimations. Traditional methods of directly calculating the distance by projecting 3D BBox to 2D BBox require a large amount of computation, so an increased number of objects tend to decline the speed of estimation during execution. Using anchor distance as a prior the proposed approach develops a computationally concise network and performs single-shot, real-time, multi-object detection even for an arbitrarily large number of objects.

## ACKNOWLEDGEMENT

We would like to thank Jihoon Moon, who gives us intuitive advice. This work is in part supported by the Air Force Office of Scientific Research under award number FA2386-17-1-4660.

## REFERENCES

- [1] R. F. Salas-Moreno, R. A. Newcombe, H. Strasdat, P. H. Kelly, and A. J. Davison, "Slam++: Simultaneous localisation and mapping at the level of objects," in *Proceedings of the IEEE conference on computer vision and pattern recognition*, 2013, pp. 1352–1359.
- [2] P. Parkhiya, R. Khawad, J. K. Murthy, B. Bhowmick, and K. M. Krishna, "Constructing category-specific models for monocular object-slam," *arXiv preprint arXiv:1802.09292*, 2018.
- [3] S. Yang and S. Scherer, "Cubeslam: Monocular 3-d object slam," *IEEE Transactions on Robotics*, vol. 35, no. 4, pp. 925–938, 2019.
- [4] S. L. Bowman, N. Atanasov, K. Daniilidis, and G. J. Pappas, "Probabilistic data association for semantic slam," in *2017 IEEE International Conference on Robotics and Automation (ICRA)*. IEEE, 2017, pp. 1722–1729.
- [5] D. F. Kevin Doherty and J. Leonard, "Multimodal semantic slam with probabilistic data association," in *2019 IEEE International Conference on Robotics and Automation (ICRA)*. IEEE, 2019.
- [6] J. Wu, Y. Wang, T. Xue, X. Sun, B. Freeman, and J. Tenenbaum, "Marnet: 3d shape reconstruction via 2.5 d sketches," in *Advances in neural information processing systems*, 2017, pp. 540–550.
- [7] H. Yu and B. H. Lee, "A variational feature encoding method of 3d object for probabilistic semantic slam," in *2018 IEEE/RSJ International Conference on Intelligent Robots and Systems (IROS)*. IEEE, 2018, pp. 3605–3612.
- [8] H. Yu, J. Moon, and B. Lee, "A variational observation model of 3d object for probabilistic semantic slam," in *2019 International Conference on Robotics and Automation (ICRA)*. IEEE, 2019, pp. 5866–5872.
- [9] Y. Xiang, W. Choi, Y. Lin, and S. Savarese, "Data-driven 3d voxel patterns for object category recognition," in *Proceedings of the IEEE Conference on Computer Vision and Pattern Recognition*, 2015, pp. 1903–1911.
- [10] A. Mousavian, D. Anguelov, J. Flynn, and J. Koščeká, "3d bounding box estimation using deep learning and geometry," in *Computer Vision and Pattern Recognition (CVPR), 2017 IEEE Conference on*. IEEE, 2017, pp. 5632–5640.
- [11] D. Proklova, D. Kaiser, and M. V. Peelen, "Disentangling representations of object shape and object category in human visual cortex: The animate–inanimate distinction," *Journal of cognitive neuroscience*, vol. 28, no. 5, pp. 680–692, 2016.
- [12] A. Mousavian, D. Anguelov, J. Flynn, and J. Kosecka, "3d bounding box estimation using deep learning and geometry," in *Proceedings of the IEEE Conference on Computer Vision and Pattern Recognition*, 2017, pp. 7074–7082.
- [13] D. P. Frost, O. Kähler, and D. W. Murray, "Object-aware bundle adjustment for correcting monocular scale drift," in *2016 IEEE International Conference on Robotics and Automation (ICRA)*. IEEE, 2016, pp. 4770–4776.
- [14] D. Frost, V. Prisacariu, and D. Murray, "Recovering stable scale in monocular slam using object-supplemented bundle adjustment," *IEEE Transactions on Robotics*, vol. 34, no. 3, pp. 736–747, 2018.
- [15] E. Sucar and J.-B. Hayet, "Bayesian scale estimation for monocular slam based on generic object detection for correcting scale drift," in *2018 IEEE International Conference on Robotics and Automation (ICRA)*. IEEE, 2018, pp. 1–7.
- [16] H. Fu, M. Gong, C. Wang, K. Batmanghelich, and D. Tao, "Deep ordinal regression network for monocular depth estimation," in *Proceedings of the IEEE Conference on Computer Vision and Pattern Recognition*, 2018, pp. 2002–2011.
- [17] J. M. Facil, B. Ummenhofer, H. Zhou, L. Montesano, T. Brox, and J. Civera, "Cam-convs: camera-aware multi-scale convolutions for single-view depth," in *Proceedings of the IEEE conference on computer vision and pattern recognition*, 2019, pp. 11 826–11 835.
- [18] D. Wofk, F. Ma, T.-J. Yang, S. Karaman, and V. Sze, "Fastdepth: Fast monocular depth estimation on embedded systems," in *2019 International Conference on Robotics and Automation (ICRA)*. IEEE, 2019, pp. 6101–6108.
- [19] F. Zhong, S. Wang, Z. Zhang, and Y. Wang, "Detect-slam: Making object detection and slam mutually beneficial," in *2018 IEEE Winter Conference on Applications of Computer Vision (WACV)*. IEEE, 2018, pp. 1001–1010.
- [20] K. He, G. Gkioxari, P. Dollár, and R. Girshick, "Mask r-cnn," in *Proceedings of the IEEE international conference on computer vision*, 2017, pp. 2961–2969.
- [21] J. Redmon and A. Farhadi, "Yolo9000: better, faster, stronger," in *Proceedings of the IEEE conference on computer vision and pattern recognition*, 2017, pp. 7263–7271.
- [22] W. Liu, D. Anguelov, D. Erhan, C. Szegedy, S. Reed, C.-Y. Fu, and A. C. Berg, "Ssd: Single shot multibox detector," in *European conference on computer vision*. Springer, 2016, pp. 21–37.
- [23] S. Ren, K. He, R. Girshick, and J. Sun, "Faster r-cnn: Towards real-time object detection with region proposal networks," in *Advances in neural information processing systems*, 2015, pp. 91–99.
- [24] B. Tekin, S. N. Sinha, and P. Fua, "Real-time seamless single shot 6d object pose prediction," in *Proceedings of the IEEE Conference on Computer Vision and Pattern Recognition*, 2018, pp. 292–301.
- [25] Y. Zhou and O. Tuzel, "Voxelnet: End-to-end learning for point cloud based 3d object detection," *arXiv preprint arXiv:1711.06396*, 2017.
- [26] A. Kundu, Y. Li, and J. M. Rehg, "3d-rcnn: Instance-level 3d object reconstruction via render-and-compare," in *Proceedings of the IEEE Conference on Computer Vision and Pattern Recognition*, 2018, pp. 3559–3568.
- [27] Y. Huo, H. Yi, Z. Wang, J. Shi, Z. Lu, P. Luo, *et al.*, "Learning depth-guided convolutions for monocular 3d object detection," in *2020 IEEE/CVF Conference on Computer Vision and Pattern Recognition Workshops (CVPRW)*. IEEE, 2020, pp. 4306–4315.
- [28] J. Zhu and Y. Fang, "Learning object-specific distance from a monocular image," in *Proceedings of the IEEE International Conference on Computer Vision*, 2019, pp. 3839–3848.
- [29] A. Simonelli, S. R. Bulo, L. Porzi, M. López-Antequera, and P. Kotschieder, "Disentangling monocular 3d object detection," in *Proceedings of the IEEE International Conference on Computer Vision*, 2019, pp. 1991–1999.
- [30] Y. Zhang, Y. Li, M. Zhao, and X. Yu, "A regional regression network for monocular object distance estimation," in *2020 IEEE International Conference on Multimedia & Expo Workshops (ICMEW)*. IEEE, 2020, pp. 1–6.
- [31] A. Bochkovskiy, C.-Y. Wang, and H.-Y. M. Liao, "Yolov4: Optimal speed and accuracy of object detection," *arXiv preprint arXiv:2004.10934*, 2020.
- [32] G. Brazil and X. Liu, "M3d-rpn: Monocular 3d region proposal network for object detection," in *Proceedings of the IEEE International Conference on Computer Vision*, 2019, pp. 9287–9296.
- [33] A. A. Soltani, H. Huang, J. Wu, T. D. Kulkarni, and J. B. Tenenbaum, "Synthesizing 3d shapes via modeling multi-view depth maps and silhouettes with deep generative networks," in *The IEEE conference on computer vision and pattern recognition (CVPR)*, vol. 3, 2017, p. 4.
- [34] J. K. Pontes, C. Kong, S. Sridharan, S. Lucey, A. Eriksson, and C. Fookes, "Image2mesh: A learning framework for single image 3d reconstruction," *arXiv preprint arXiv:1711.10669*, 2017.
- [35] Z. Liu, Z. Wu, and R. Tóth, "Smoke: Single-stage monocular 3d object detection via keypoint estimation," in *Proceedings of the IEEE/CVF Conference on Computer Vision and Pattern Recognition Workshops*, 2020, pp. 996–997.
- [36] M. Simony, S. Milzy, K. Amendey, and H.-M. Gross, "Complex-yolo: An euler-region-proposal for real-time 3d object detection on point clouds," in *Proceedings of the European Conference on Computer Vision (ECCV)*, 2018, pp. 0–0.
- [37] A. Geiger, P. Lenz, and R. Urtasun, "Are we ready for autonomous driving? the kitti vision benchmark suite," in *Computer Vision and Pattern Recognition (CVPR), 2012 IEEE Conference on*. IEEE, 2012, pp. 3354–3361.
- [38] Z. Zheng, P. Wang, W. Liu, J. Li, R. Ye, and D. Ren, "Distance-iou loss: Faster and better learning for bounding box regression," 2019.
- [39] F. Gökçe, G. Üçoluk, E. Şahin, and S. Kalkan, "Vision-based detection and distance estimation of micro unmanned aerial vehicles," *Sensors*, vol. 15, no. 9, pp. 23 805–23 846, 2015.
- [40] S. Tuohy, D. O’Cualain, E. Jones, and M. Glavin, "Distance determination for an automobile environment using inverse perspective mapping in opencv," 2010.